

## Electronic Supplementary Information

### *Active Colloidal Microdrills*

Submitted to Chemical Communications (2015)

J. G. Gibbs<sup>†a,b</sup> and P. Fischer<sup>a,c</sup>

<sup>a</sup>Max Planck Institute for Intelligent Systems, Heisenbergstr. 3, 70569 Stuttgart, Germany.

<sup>b</sup>Department of Physics and Astronomy, Northern Arizona University, S San Francisco St.,  
Flagstaff, AZ 86011, United States.

<sup>c</sup>Institute for Physical Chemistry, University of Stuttgart, Pfaffenwaldring 55, 70569  
Stuttgart, Germany.

†john.gibbs@nau.edu

### Table of contents

S1	Deposition procedure
S2	Helix critical dimensions
S3	Experimental procedure
S4	Video explanations
S5	Driving force
S6	Additional SEM images
S7	Data for Fig. 4 (main text)
S8	Diffusion coefficient for Brownian motion
S9	Additional references

## S1. Deposition Procedure

First 1  $\mu\text{m}$   $\text{SiO}_2$  beads were deposited onto clean Si(100) wafers by drop casting mixtures of beads and ethanol (1:5). The wafers are then placed into a vacuum chamber of pressure  $P \sim 10^{-6}$  Torr. The sub-monolayer served as points of growth for glancing angle deposition (GLAD).<sup>1</sup> The substrate is tilted to an oblique angle  $\alpha = 85^\circ$  with respect to the incoming vapour, i.e.  $\alpha = 0^\circ$  (normal incidence) would give a thin film. In order to properly deposit the Pt onto the back side of the helix, one single helix turn was first deposited by slowly rotating the substrate during deposition at a rate determined by the deposition thickness monitored by a quartz crystal microbalance. Once the first turn was deposited with  $\text{SiO}_2$ , the substrate was tilted back to  $\alpha = 0^\circ$  and a thin layer of 3 nm Ti was deposited as an adhesion layer. After this step, with the tilt angle still  $\alpha = 0^\circ$ , a layer of 10 nm of Pt was deposited. Next, the substrate angle was returned to  $\alpha = 85^\circ$ , at which time the second helix single-turn was added and the total process was repeated 3 times. It should be noted that with the substrate at  $\alpha = 85^\circ$ , 3 nm of Ti was added to ensure that each subsequent single-turn helix would properly adhere to the former. The final morphology is shown in the main text and the supplementary SEM images of Fig. S4 shown of this SI.

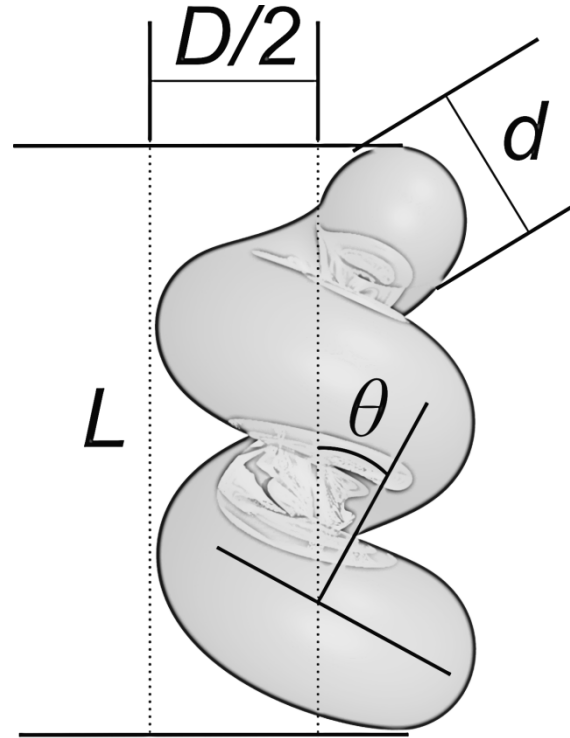


**Fig. S1** Schematic of the helical swimmer showing the critical dimensions: length, major diameter, minor diameter, and angle as  $L$ ,  $D$ ,  $d$ , and  $\theta$  respectively.

## S2. Helix critical dimensions

Measurements made were made with SEM (10 measurements each), based upon the scale bar given by the machine.

Length,  $l = 5460, 5298, 5570, 4840, 5216, 5461, 4972, 5570, 5623, 5407$  nm.

$\bar{l} = 5300 \pm 300$  nm (average).

Major diameter,  $D: 1621, 1216, 1135, 1459, 1405, 1595, 1486, 1865, 1459, 1297$  nm.

$\bar{D} = 1400 \pm 200$  nm.

Minor diameter,  $d = 573, 741, 498, 653, 624, 663, 663, 667, 548, 653$  nm.

$\bar{d} = 630 \pm 70$  nm.

Length of pitch,  $p = 1270, 1459, 1351, 1270, 1432, 1324, 1276, 1352, 1216, 1299$  nm.  
 $\bar{p} = 1330 \pm 80$ .

Thread angle:  $\theta = 29, 33, 29, 34, 28, 32, 29, 28, 39, 42^\circ$   
 $\bar{\theta} = 32 \pm 5^\circ$

**Table S1.** Types of swimming behaviours observed.

Type	Number	%
Screw	31	23.1
Circle	31	23.1
End over end	33	24.6
Translational	14	10.4
Perp. Spin	15	11.2
Other	10	7.5

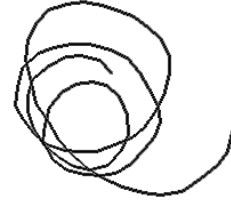


**Fig. S2** Trajectory of circular swimming behaviour for SI video V2.

### S3. Experimental Procedure

Videos were taken of the autonomous screws using a Basler camera ACE on a Zeiss Axiophot microscope. A  $50 \times$  objective was used in reflection mode since the movement was observed on opaque Si wafers. All videos are of particles moving very close to the surface of a substrate as determined by the position of the focal plane. Videos with the Basler camera were taken at  $\sim 20$  frames per second (fps), with a scale of 9.3 pixels/micron.

### S4. Videos

V1. Video showing a single microdrill undergoing Brownian motion (in  $H_2O$  only) on the surface of the Si wafer.

V2. Video also showing a single microdrill undergoing Brownian motion but using dark field microscopy to show the metallic coating.

V3. Video showing a single circle swimmer.

V4. Video showing a single end over end motion.

V5 ... translational

V6 ... spinning

V7 ... rotation suppression near the surface

V8 – V12 videos showing microscrew motion (rotation and translation)

### S5. Force considerations

It has been clearly demonstrated that for an electrical insulator-based catalytic motor, that the motion is away from the catalyst.<sup>2</sup> Because the subsequent deposition of the SiO<sub>2</sub> partially covers the Pt from the previous deposition step, there is a slight asymmetry to the distribution of the Pt as shown in the SEM of Fig. S3. This leads to a transverse force which explains why one of the most common swimming types is circular (translation with no rotation). For the screw motors, as one half turn is completed, this transverse effect is easily seen in the motion. That is, the screw is pushed laterally in one direction, then the other after one-half turn. The force has both an axial and lateral components. The asymmetry results in not only a force leading to translational motion, but a driving torque as well. Both this driving torque and the torque due to drag both result in microdrill motion. Additional SEM images are given in Fig. 4.

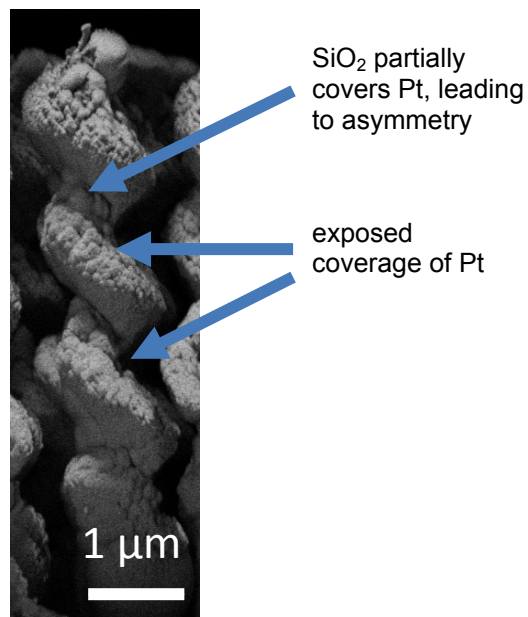


**Fig. S3** Location of the Pt catalyst on the SiO<sub>2</sub> helical backbone.

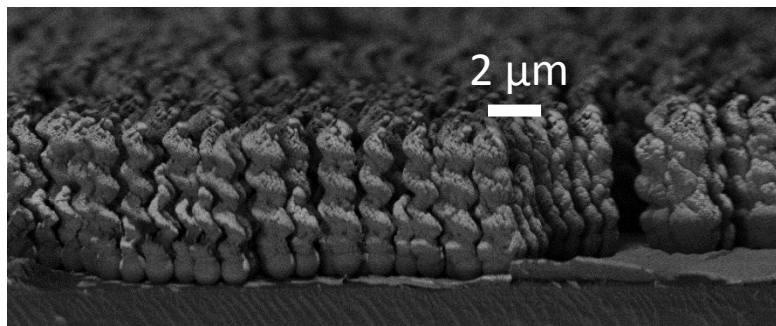
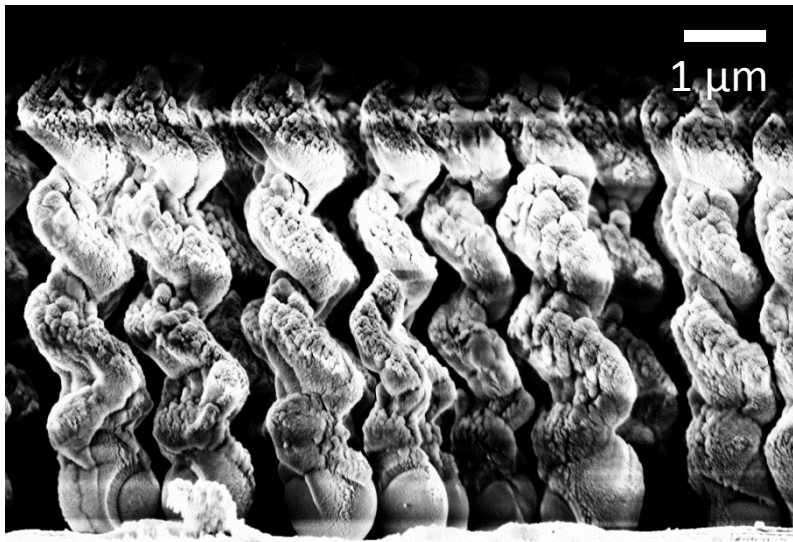
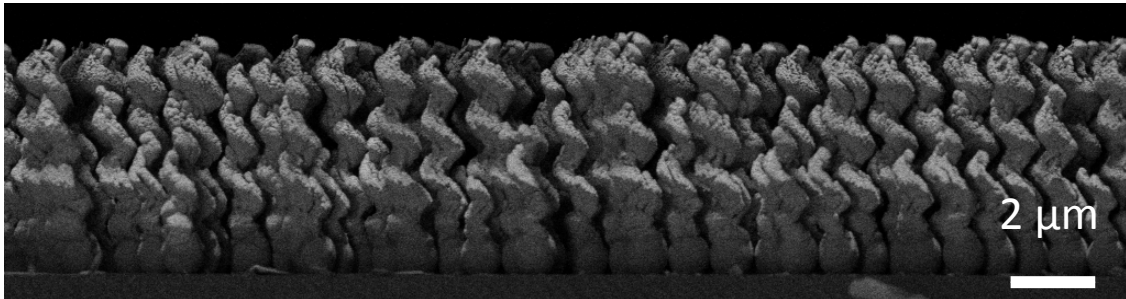


**Fig. S4** Additional SEM images showing arrays of catalytic screws after deposition using GLAD

## S6. Additional SEM images

## S7. Data for swimmer in Fig. 4 of main text

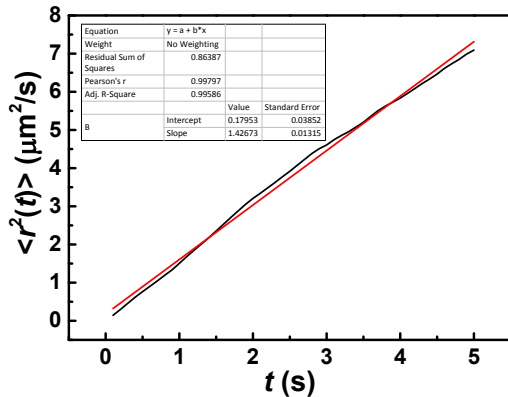
The total length of this particle  $l = 3.1 \mu\text{m}$ .  $\bar{p} = 1330 \pm 80 \text{ nm}$ . The table below shows the

Time	distance pix.	$\Delta t$ (s)	$d$ ( $\mu\text{m}$ )
0.95	33.1	-	3.6
1.21	42.2	0.26	4.5
1.42	40.4	0.21	4.3
1.68	48.9	0.26	5.3
2	52.9	0.32	5.7
2.32	53.7	0.32	5.8
2.68	54.1	0.34	5.8
3.05	69.1	0.37	7.4
3.26	43.4	0.21	4.7
3.53	47.3	0.27	5.1
-	$\bar{p}_{ix} = 49 \pm 10$	$\bar{\Delta t} = 0.28 \pm 0.06$	$\bar{d} = 5 \pm 1$

**Table S2.** Data for a single swimmer shown in Fig. 5 of the main text.

measurements of the distance travelled and the amount of time required for one half turn. The data was measured in pixels and converted to actual distance.

## S8. Diffusion coefficient for Brownian motion



Brownian motion for 5 particles. The linear fit gives a slope of  $1.42 \pm 0.013$ ,  $\text{MSD} = 4Dt$  in 2D:  $0.355 \mu\text{m}^2/\text{s}$ . The diffusion coefficient (for a sphere) or radius  $R$  is given by  $D = kBT/6\pi\eta R$ , in which  $kBT$  is the energy, and  $\eta$  is the fluid viscosity.

## S9. Additional References

- 1 K. Robbie and M. Brett, *Journal of Vacuum Science & Technology A*, 1997, **15**, 1460; Y.-P. Zhao, D.-X. Ye, G.-C. Wang and T.-M. Lu, *Nano Letters*, 2002, **2**, 351.
- 2 J. Gibbs and Y.-P. Zhao, *Applied Physics Letters*, 2009, **94**, 163104.

